Journal of Controlled Release 286 (2018) 439–450

Contents lists available at ScienceDirect

Journal of Controlled Release

journal homepage: www.elsevier.com/locate/jconrel

Intradiscal delivery of celecoxib-loaded microspheres restores intervertebral disc integrity in a preclinical canine model

A.R. Tellegen[a], I. Rudnik-Jansen[b], M. Beukers[a], A. Miranda-Bedate[a], F.C. Bach[a], W. de Jong[a], N. Woike[c], G. Mihov[c], J.C. Thies[c], B.P. Meij[a], L.B. Creemers[b], M.A. Tryfonidou[a,*]

[a] Department of Clinical Sciences of Companion Animal Medicine, Faculty of Veterinary Medicine, Utrecht University, The Netherlands
[b] Department of Orthopedics, University Medical Centre Utrecht, The Netherlands
[c] DSM Biomedical, Geleen, The Netherlands

ARTICLE INFO

Keywords:
Controlled release
Polyesteramide microspheres
Chronic low back pain
MRI
Inflammation
Subchondral bone

ABSTRACT

Low back pain, related to degeneration of the intervertebral disc (IVD), affects millions of people worldwide. Clinical studies using oral cyclooxygenase-2 (COX-2) inhibitors have shown beneficial effects, although side-effects were reported. Therefore, intradiscal delivery of nonsteroidal anti-inflammatory drugs can be an alternative treatment strategy to halt degeneration and address IVD-related pain. In the present study, the controlled release and biologic potency of celecoxib, a selective COX-2 inhibitor, from polyesteramide microspheres was investigated *in vitro*. In addition, safety and efficacy of injection of celecoxib-loaded microspheres were evaluated *in vivo* in a canine IVD degeneration model. *In vitro*, a sustained release of celecoxib was noted for over 28 days resulting in sustained inhibition of inflammation, as indicated by decreased prostaglandin E_2 (PGE_2) production, and anti-catabolic effects in nucleus pulposus (NP) cells from degenerated IVDs on qPCR. *In vivo*, there was no evidence of adverse effects on computed tomography and magnetic resonance imaging or macroscopic evaluation of IVDs. Local and sustained delivery of celecoxib prevented progression of IVD degeneration corroborated by MRI, histology, and measurement of NP proteoglycan content. Furthermore, it seemed to harness inflammation as indicated by decreased PGE_2 tissue levels and decreased neuronal growth factor immunopositivity, providing indirect evidence that local delivery of a COX-2 inhibitor could also address pain related to IVD degeneration. In conclusion, intradiscal controlled release of celecoxib from polyesteramide microspheres prevented progression of IVD degeneration both *in vitro* and *in vivo*. Follow-up studies are warranted to determine the clinical efficacy of celecoxib-loaded PEAMs in chronic back pain.

1. Introduction

Low back pain is the most common type of pain restricting daily activity and has a huge impact on quality of life and productivity [1, 2]. Due to the aging population and lifestyle changes, the burden on society will even continue to increase. Neck or back pain is associated with intervertebral disc (IVD) degeneration in a substantial part of the patients [3]. Genetic predisposition, mechanical overload, and unhealthy lifestyle can contribute to and aggravate degeneration of the IVD [4]. Increasing evidence points to a role for pro-inflammatory mediators in the degenerative process and to pain on a molecular level [5]. The latter occurs through several mechanisms. Pro-inflammatory mediators promote catabolic changes that lead to loss of proteoglycans in the core of the IVD, the nucleus pulposus (NP), resulting in a dehydrated disc with less shock-absorbing properties [6–8]. These biomechanical changes eventually lead to spinal instability and decreased disc height, with subsequent compression of nerves, exiting the intervertebral foramen. Tears and clefts appear in the degenerating annulus fibrosus (AF), the fibrous ring constraining the NP, and the disc can bulge into the spinal canal, leading to compression of neural tissues. Furthermore, in the degenerating IVD, blood vessels and nerve endings can penetrate the normally avascular and aneural IVD, *via* the production of neurotropic and angiogenic factors such as nerve growth factor (NGF) and vascular endothelial growth factor [5, 8–12]. This process is driven by pro-inflammatory mediators such as the cyclooxygenase-2 (COX-2) derived prostaglandin E_2 (PGE_2) and can, even in the absence of the aforementioned changes, contribute to discogenic pain [13]. Given that pain related to IVD degeneration may have multiple routes mediated by inflammation, oral anti-inflammatory drugs are being widely used in the clinic.

* Corresponding author at: Faculty of Veterinary Medicine, Yalelaan 108, 3584 CM Utrecht, The Netherlands.
E-mail address: m.a.tryfonidou@uu.nl (M.A. Tryfonidou).

https://doi.org/10.1016/j.jconrel.2018.08.019
Received 25 April 2018; Received in revised form 9 August 2018; Accepted 10 August 2018
Available online 12 August 2018

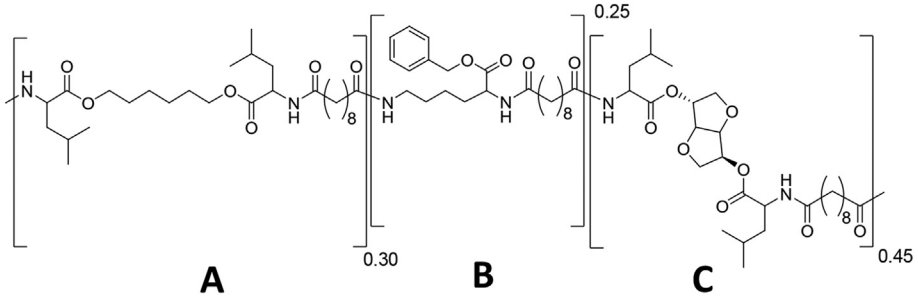

Fig. 1. Structure of polyesteramide (PEA) III Ac Bz random copolymer consisting of building blocks A, B and C (Leu, Lys, Leu).

Current therapies for neck and back pain merely focus on pain management. To achieve biologic repair, novel treatment strategies also aim at inhibiting the degenerative process and restoring tissue integrity [14, 15]. They are challenged by the fact that tissue penetration of orally administered drugs into the avascular IVD is limited [16, 17]. To this end, local delivery of stem cells and/or drugs seems to be a feasible strategy for the treatment of symptomatic IVD degeneration. Intradiscal transplantation of mesenchymal stromal cells (MSCs), although effective in treating pain, is challenged by high costs and the limited capacity of MSCs in enhancing IVD regeneration in clinical trials [18]. Drugs could provide a cost-effective alternative. Hereby, drug delivery systems enable drug loading at a higher dose and effectuate sustained drug release over prolonged period of time. Specifically for intradiscal application, such systems enable the development of minimally invasive treatment strategies keeping re-injections to a minimum; thereby supporting disc homeostasis while enabling biologic repair.

The evolution of resorbable degradable polymers from aliphatic polyesters to nitrogen bearing polymers such as polyurethanes, polyester amides and polyureas has been accompanied with better control over degradation and release properties. In addition, incorporation of amino acid-based building blocks provide one or more functional groups along the polymer chain that allow further modification of the polymer to tailor its physicochemical properties and performance as drug eluting matrices [19, 20]. Microspheres based on biodegradable polyesteramide (PEA) polymers are a promising biomaterial platform for local drug delivery. These amino acid-based polymers provide good thermal and mechanical properties [21]. The polymer has been built of three di-amino monomers connected with di-acid linker in a polycondensation reaction. The monomer composition results in specific ester to amide bonds ratio which is essential for polymer biodegradation [19, 20]. An important advantage of these polymers is related to the fact that they predominantly degrade *via* an enzymatic mechanism and due to consequential surface erosion, drug release follows unique release kinetics [20], allowing for constant drug release in the degenerative IVD environment. PEA microspheres (PEAMs) can in this way serve as an autoregulatory drug delivery system [22]. In an inflammatory environment such as the osteoarthritic knee joint and degenerated IVD [23], proteases are abundantly present, leading to increased microsphere degradation and thus, faster drug release, harnessing inflammation. Recently, PEAMs have been shown to be safe for intradiscal application in a canine model predisposed to IVD degeneration, when employed with small needle sizes and limited injection volumes [24]. However, not much is known regarding optimal drug loading dose in a controlled release system for the degenerated IVD to achieve biologic repair.

The overall aim of the present study was to translate local controlled delivery of a COX-2 inhibitor for the purpose of biologic disc repair employing a clinically relevant animal model. Naturally occurring IVD degeneration in dogs resembles IVD degeneration in man with similar molecular, histological, radiological, and clinical characteristics. The dog is therefore a valuable translational large animal model for human and veterinary patients with chronic back pain [14, 25]. The biologic potency of controlled release of celecoxib on canine NP cells from degenerated IVDs, was first evaluated *in vitro*. Thereafter, safety and efficacy of a single intradiscal injection of PEAMs loaded with celecoxib in a dose range of 0.2–7 mg/mL corresponding to 10^{-4} M and 10^{-2} M total injected celecoxib, respectively, was evaluated *in vivo* employing a combination of diagnostic imaging, biochemical, and histological read out parameters.

2. Material and methods

2.1. Synthesis and characterization of particle size, particle morphology, loading efficiency and release of celecoxib from polyesteramide microspheres

2.1.1. Synthesis and characterization of the polymer

The biomaterial in this study was a biodegradable poly(esteramide) based on α-amino acids, aliphatic dicarboxylic acids and aliphatic α-ω diols. The selected PEA comprises three types of building blocks randomly distributed along the polymer chain (Fig. 1). The polymer was synthesized according to a procedure reported previously [26]. Briefly, the polymer was prepared *via* solution polycondensation of di-p-toluenesulfonic acid salts of bis-(α-amino acid) α,ω- diol diesters, lysine benzyl ester and di-N-hydroxysuccinimide sebacate in anhydrous DMSO. The use of pre-activated acid in the reaction allows polymerization at low temperature (65 °C) affording side-product free polycondensates and predictable degradation products. The polymer was isolated from the reaction mixture in two precipitation steps. ^{1}H nuclear magnetic resonance (NMR) spectra were obtained on a Bruker Avance 500 MHz Ultrashield NMR; samples were recorded in DMSO d_6. Molecular weight and molecular weight distributions of PEA were determined by gel permeation chromatography equipped with refractive index detector. Samples were dissolved in tetrahydrofuran at a concentration of approximately 5 mg/mL and were run at a flow rate of 1 mL/min at 50 °C. The molecular weights were calibrated to a narrow polystyrene standard calibration curve, using Waters Empower software.

2.1.2. Microsphere preparation

Polyesteramide polymer was dissolved in dichloromethane (15wt/v %). To generate celecoxib (CXB) loaded PEAMs, the drug was added (Polymer: dichloromethane 5 wt%). After homogenization, the solution was sonicated in a water bath for 3 min. The PEA-CXB solution was then emulsified in 20 mL of water phase (PVA 1 wt%, NaCl 2.5 wt%) by the use of an ultraturrax, stirring at 4000 rpm (8000 rpm for empty PEAMs) for 3 min. After emulsification, particles were hardened overnight under air flow. Before washing, particles were cooled with an ice-bath for 1 h and washed with Tween 80. Excess of surfactant was removed by centrifugation. Before freeze-drying to remove residual solvent, particles were suspended in Tween 80 in order to reach the right concentration of particles per volume: 1.05 and 35 mg particles/mL for CXB-loaded PEAMs, with 20 wt% CXB in the loaded PEAMs. For the unloaded particles, a 35 mg/mL concentration was prepared. Once dried, the PEAMs were weighted in individual HPLC vials to the

Table 1
Details on polyesteramide microspheres used in the *in vivo* study. CXB, celecoxib; LD, low dose; HD, high dose.

Condition	Size distribution		Loading (wt %)	Particle concentration (mg/mL)
	D(0.5) (μm)	Span		
Unloaded	31.9	1.168	0	35
LD-CXB	25.3	1.14	20	1.05
HD-CXB	25.3	1.14	20	35

approximate amount of 1.05 or 35 mg PEAMs corresponding with 0.2 and 7 mg CXB, respectively, and γ-sterilized on dry ice (Table 1). The loading dose of the particles was chosen based on restrictions for the injectable volume to a degenerating disc and a previous study investigating the controlled release of 0.38–38 μg CXB per mL in a dose response fashion from a pNIPAAM hydrogel [27]. Provided that only mild PGE_2 inhibition was observed *in vivo* in the latter study, a much higher CXB loading dose was chosen in the present *in vivo* study.

2.2. Release kinetics of celecoxib-loaded polyesteramide microspheres in PBS

Drug loading of CXB was determined by weighing ~15 mg of microparticles and dissolving them in methanol:PBS (75:25 v/v). Samples were filtered over 0.45 μm Teflon filter and diluted towards an amount that fits within the middle range of calibration standards (0.1 μg/mL-20 μg/mL). Release of celecoxib from the PEAMs in PBS for 14 days was measured by HPLC as described previously [22]. Briefly, at least 15 mg of microspheres with 20% celecoxib loading were placed in centrifuge tubes and immersed in 40 mL phosphate buffered saline (PBS) at 37 °C under gentle shaking. After centrifugation, 36 mL buffer was removed and replaced with the same amount of fresh buffer at defined timepoints such as 2 h, 5 h, day 1, day 2, 3, 4, 7, 8, 9, 11 and 14 days until completion of the release study. Release was stopped after 14 days release and mass balance was determined. After the last removal of buffer at 14 days, particles were washed with 10 mL of water to remove the remaining PBS buffer. Particles were centrifuged, and 15 mL of water was removed. This step was repeated three times. Particles were then dried in the oven under full vacuum and ambient condition for 48 h. Particles were dissolved with methanol:PBS (75:25 *v*/v) mixture and measured with HPLC.

2.3. The effect of PEA based celecoxib-loaded microspheres on nucleus pulposus cells in vitro

2.3.1. Setup of in vitro experiment

The anti-inflammatory effects of the CXB-loaded PEA platform on canine NP cells, in the presence of the pro-inflammatory stimulus TNF-α (10 ng/mL), was tested in monolayer culture as a measure of the bioactivity of the released celecoxib (Fig. 2A). NP tissue was collected *post-mortem* from the (untreated) cervical spine of the dogs described in the *in vivo* experiment, in aseptic conditions. The cervical spine had received no treatment during the *in vivo* experiment. Thereafter, NPs were digested by 0.15% *w/v* pronase for 45 min (10,165,921,001, Roche Diagnostics) and 0.15% w/v collagenase overnight (LS004177, Worthington). Cells were expanded in hgDMEM + Glutamax (31,966, Gibco Life Technologies) containing 10% *v*/v FBS (16000–044, Gibco Life Technologies), 1% v/v penicillin/streptomycin (p/s, P11–010, PAA laboratories), 0.1 mM ascorbic acid 2-phosphate (Asap, A8960, Sigma-Aldrich), 10^{-9} M dexamethasone (D1756, Sigma-Aldrich), 1 ng/mL basic fibroblast growth factor (PHP105, AbD Serotec), and 0.05% *v*/v fungizone (15290–018, Invitrogen) at 37 °C, 21% O_2 and 5% CO_2. The culture medium was renewed every 3–4 days. At passage two, NP cells were cryopreserved in aliquots of 10^6 cells per vial in hgDMEM + Glutamax with 10% *v*/v DMSO (20–139, EMD Millipore Corporation) and 10% v/v FBS. Three days before the experiment, cells were thawed and seeded on a 24-wells plate (662,160, Greiner bio-one) at a density of 60,000 cells per well under hypoxic conditions (5% O_2). Cells were cultured in chondrogenic medium (hgDMEM + Glutamax) containing 1% v/v p/s, 1% v/v ITS + premix (354,352, Corning Life Sciences), 0.04 mg/mL L-proline (P5607, Sigma-Aldrich), 0.1 mM Asap and 1.25 mg/mL bovine serum albumin (A9418, Sigma-Aldrich).

On day 0, the medium was renewed and the unloaded or CXB-loaded PEAMs were dispersed in chondrogenic culture medium and placed in Transwell® baskets (pore size 0.4 μm, polycarbonate membrane, Costar Corning) (Fig. 2A). Two concentrations of CXB-loaded microspheres were utilized: 1.33 μg/mL and 1.33 mg/mL, corresponding with 10^{-7} M and 10^{-4} M celecoxib in order to achieve partial and complete inhibition of COX-2 activity within the culture system and thereby determine dose-dependent bioactivity. Cells and microspheres were co-incubated for 4 h at 37 °C, 5% CO_2 and 95% humidity. Subsequently, a pro-inflammatory stimulus was provided by adding 10 ng/mL TNF-α (R&D Systems, Oxon, United Kingdom). Cells treated with a celecoxib bolus (equivalent to 10^{-6} M), were included as positive controls at each time interval. For determination of celecoxib bioactivity, NP cells and microspheres were co-incubated for 72 h before the microspheres were transferred to a new 24-well culture plate containing cells seeded according to the procedure described above ($n = 6$ donors, in duplicates). This procedure was repeated 8 times amounting to a release period of 28 days. Every 72 h, medium was collected and stored at −80 °C.

2.3.2. In vitro read out parameters

In medium, PGE_2 levels were measured using the enzyme immunoassay PGE_2 EIA Kit (514,010, Cayman Chemical), according to the respective manufacturer instructions. Celecoxib was measured using a competitive colometric ELISA (180,719, Neogen Corp) following manufacturer's instructions. DNA content was measured using the Qubit® dsDNA High Sensitivity Assay Kit (Q32851, Invitrogen). RNA was isolated using the RNeasy® microkit (74,004, Qiagen) according to the manufacturer's instructions, including a DNAse (RNAse-Free DNase Set, 79,254, Qiagen) step. cDNA was synthesized using the iScript™ cDNA Synthesis Kit (170–8891, Bio-Rad) according to the manufacturer's instructions. Primer sequences were designed using PerlPrimer (Supplementary file 1). RT-qPCR was performed using the iQT™ SYBR Green Supermix Kit and the CFX384 Touch™ Real-Time PCR Detection System (both from Bio-Rad). For determination of relative gene expression, the Normfirst ($E^{\Delta\Delta Cq}$) method was used. For each target gene, the mean n-fold changes and standard deviations in gene expression were calculated. Four reference genes shown to be stable were chosen to normalize gene expression of target genes (Supplementary File 1).

2.4. In vivo experimental design

Animal experiments were approved and conducted in accordance with guidelines of the Animal Experiments Committee (project number AVD108002015282), as required by Dutch regulation. All animal experiments were conducted in compliance with the standards of animal care of the Faculty of Veterinary Medicine. Six healthy intact male dogs were purchased from Marshall BioResources (19 months of age, body weight 8–10 kg). In line with the reduction and refinement of experimental animal use, the dogs were employed for the study of two anti-inflammatory agents loaded on PEAMs, one of which was celecoxib, which is reported here. Three dogs were used in the current study. Controls, *i.e.* unloaded PEAMs, were shared between these two experiments, resulting in a total of $n = 6$ IVDs per condition.

Intervertebral disc degeneration was induced at five alternating levels (T12-T13, L1-L2, L3-L4, L5-L6 and L7-S1; see below). Four weeks after induction of degeneration, magnetic resonance imaging (MRI) was performed to assess IVD degeneration at baseline. Thereafter, CXB-

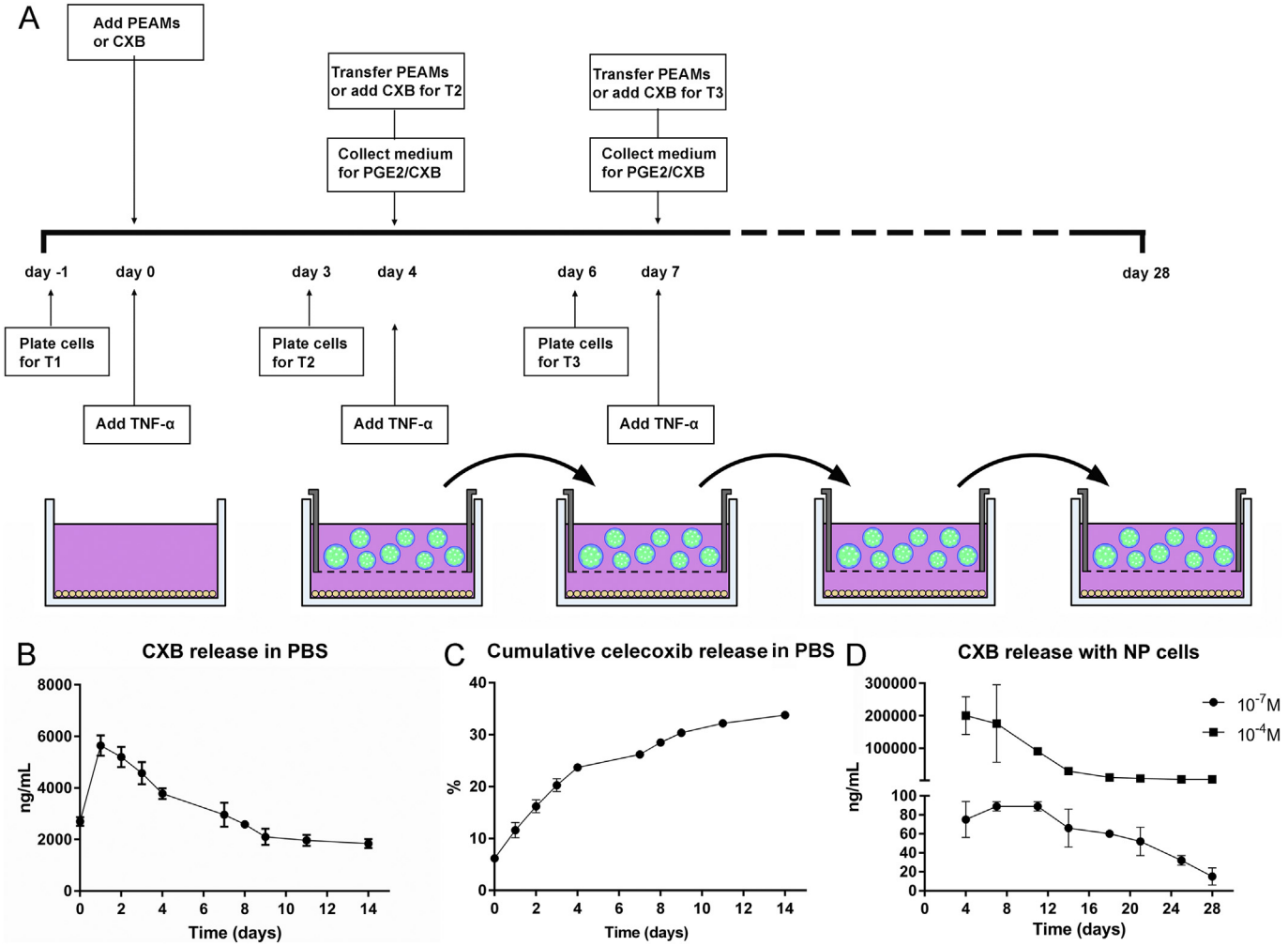

Fig. 2. Controlled release of celecoxib *in vitro*. A. Schematic overview of *in vitro* celecoxib (CXB) release from polyesteramide microspheres (PEAMs) in the presence of nucleus pulposus (NP) cells from degenerated canine intervertebral discs (A). $n = 6$ donors per condition per time point, in technical duplicates. Absolute (B) and (C) cumulative CXB release in PBS: after 14 days, approximately 30% was released. $n = 3$ per time point. (D) Absolute CXB release from PEAMs containing CXB resulting into a final concentration of 10^{-7} M and 10^{-4} M CXB loaded on the PEAMs in the presence of NP cells: after 28 days, ~20% and 40% was released respectively, from the 10^{-7} M and 10^{-4} M loaded PEAMs. $n = 2$ per time point.

loaded and empty PEAMs were injected in a random fashion with $n = 6$ IVDs per experimental group (*i.e.* non-induced IVDs, unloaded PEAMs (control, $n = 6$ dogs), and low dose (LD) and high dose (HD) CXB-loaded PEAMs both as duplicates in $n = 3$ dogs). Twelve weeks thereafter, MRI was performed, and the dogs were sacrificed with intravenous (IV) administration of pentobarbital (200 mg/kg). *Post-mortem*, computed tomography (CT) of the lumbar spine was performed. Subsequently, the spinal column was harvested, and spinal units were collected as described previously [27] and further processed for macroscopic and histopathologic assessment and for biochemical analysis. Briefly, each spinal unit (½ vertebra – IVD – ½ vertebra) was mid-sagitally transected. One half of the IVD tissue containing (NP and AF) was snap frozen in liquid nitrogen and stored at −80 °C until further biochemical analyses. The other part was photographed for macroscopic evaluation (Thompson score) and fixed in 10% buffered formaldehyde.

2.4.1. Surgical induction of intervertebral disc degeneration

Degeneration of the IVD was achieved by the method described by Hiyama et al. [28]. Pre-operative analgesia was secured by IV administration of 4 mg/kg carprofen and 20 μg/kg buprenorphine. Premedication consisted of 10 μg/kg dexmedetomedine IV anesthesia was subsequently induced with 1–2 mg/kg propofol IV. The dogs received endotracheal tubes and general anesthesia was maintained by 1–1.5% *v*/v isoflurane gas, delivered in a 1:1 oxygen:air mixture. Peri-operative analgesia consisted of continuous rate infusion (CRI) of ketamine (10 μg/kg/min) and dexmedetomedine (2 μg/kg/h). Throughout the complete procedure heart rate, respiration rate, body temperature, carbon dioxide and oxygen levels were monitored. The dogs were positioned in a right recumbent position and the surgical area was prepared aseptically to expose the left lateral AF of T12-T13 until the L5-L6 IVDs. The skin was incised and the IVDs were localized, an 18G needle was inserted superficially on the AF perimeter to check the location of the needle by intra-operative fluoroscopy. When correct needle placement was confirmed, the needle was inserted through the AF into the center of the NP and with a 10 mL syringe, the NP was aspirated. The L7-S1 IVD was approached dorsally in a percutaneous fashion, and correct needle placement on and through the dorsal AF was again confirmed by fluoroscopy. Postoperative analgesia consisted of subcutaneous administration of carprofen (4 mg/kg, q24h) and intramuscular (IM) administrations of buprenorphine (20 μg/kg q8h) for 3 days. Dogs were monitored daily in the first week postoperatively by a veterinarian (AT).

2.4.2. Intradiscal injection of PEAMs

Four weeks after induction of IVD degeneration, PEAMs were

injected directly into the center of the IVD employing the same anesthesia protocol as was used for the induction of IVD degeneration. Pre- and postoperative analgesia consisted solely of buprenorphine, to exclude the possibility of carprofen interfering in the study after CXB-PEAM injections. Intradiscal injections were performed with 100 μL gastight Hamilton syringes (7656–01 Model 1710 RN, Hamilton Company USA) connected to 27 G needles (25 mm, 12° beveled point; Hamilton Company USA). Per IVD, 40 μL was injected, a volume shown to be safe and not to induce further degeneration in this animal model [24, 29]. Approach of the IVDs was identical to the induction procedure, on the contralateral side. In each dog, unloaded PEAMs were injected in the T12-T13 disc. In the other IVDs, high (280 μg CXB/ 40 μL) and low (8.4 μg CXB/ 40 μL) doses of PEAMs loaded with CXB were injected in a random fashion, with $n = 2$ per condition per dog.

2.4.3. Diagnostic imaging

MR images were obtained to assess the degree of degeneration, *i.e.* 4 weeks after induction of IVD degeneration, just prior to intradiscal injection of biomaterials, and repeated 12 weeks after treatment. The dogs received dexmedetomedine (10 μg/kg IV) and butorphanol (0.1 mg/kg) as premedication. General anesthesia was induced by IV administration of 1–2 mg/kg propofol. General anesthesia was maintained by CRI of propofol (5 mg/kg/h IV) and dexmedetomedine (2 μg/kg/h IV). An oxygen:air mixture was provided *via* an endotracheal tube. Throughout the complete procedure heart rate, respiration rate, CO2 and O2 levels were monitored. Dogs were positioned in dorsal recumbency. MR images were obtained using a high field 1.5 T MRI unit (Ingenia, Philips, Best, The Netherlands). Sagittal T1-weighted Turbo Spin Echo (repetition time (TR) = 400 ms, echo time (TE) = 8 ms), and T2-weighted Turbo Spin Echo (TR = 3000, TE = 110 ms) images were acquired using a field of view (FOV) of 75 × 220 mm and acquisition matrix of 124 × 313 and 124 × 261, respectively. Thirteen slices of 2 mm covered the spine from Th10 to the sacrum. For T2 mapping, a quantitative multiple spin-echo T2 mapping sequence was used with the following parameters: FOV = 75 × 219 mm, acquisition matrix = 96 × 273, slice thickness = 3 mm, TR = 2000. Eight echoes were acquired with TE = 13 to 104 ms with 13 ms echo spacing. Sagittal T1ρ-weighted imaging was performed using a spin-lock-prepared sequence with a three-dimensional multi-shot gradient echo (T1-TFE) readout with the following parameters: FOV = 76 × 220 mm, acquisition matrix = 76 × 220 slice thickness = 2 mm, TR/TE = 4.6 s /2.3, TR = 5 ms, TE = 2.5 ms, TFE factor = 50, flip angle = 45°, shot interval = 3000 ms. To allow quantitative T1ρ mapping, data were acquired with different spin-lock times (TSL) of 0, 10, 20, 30 and 40 ms, with a spin-lock pulse amplitude set to 500 Hz. An oval region of interest (ROI) was manually segmented on the NP of all spinal segments in the mid-sagittal slice. T2 and T1ρ values were computed by voxel-wise fitting and calculating the mean signal intensity (S) in each ROI, using the Levenberg-Marquardt nonlinear least-squares method as described before [27]. Twelve weeks after PEAM injection, the MRI was repeated and the dogs were subsequently euthanized. *Post-mortem* CT scans with dogs positioned in dorsal recumbency were made with a 64-slice CT scanner (Siemens Somatom Definition AS, Siemens Healthcare) using the following parameters: 0.6 mm slice thickness, 120 kV, 350 mAs, 1000 ms tube rotation time, 0.35 spiral pitch factor, 512 × 512 pixel matrix and a fixed field of view of 93 mm. Reconstructions of 0.6 mm thick slices were made in a transverse and sagittal plane using soft tissue and bone reconstruction kernels. Images were reviewed in soft tissue (window width 300, window length 50) and bone (window width 3000, window length 600) settings. From T12 to S1, all IVDs were graded (AT, IR) according to the Pfirrmann score previously validated for use in dogs by Bergknut et al. [30] on T2-weighted images. Presence and classification of sclerosis of the end plates and Modic changes were recorded by a board-certified radiologist (MB), and the Disc height index (DHI) of all IVDs in the study was calculated for all IVDs on T2-weighted MR images (AT, IR) [31].

2.4.4. Macroscopic grading, histopathological grading and collagen immunohistochemistry

Digital images of the IVD segments were evaluated in random order by two blinded investigators (AT, IR) according to the Thompson grading scheme, validated for dogs previously by Bergknut et al. [32]. Tissues were fixed at room temperature (RT) for 14 days and were subsequently decalcified in 0.5 M ethylenediaminetetraacetic acid (EDTA) at RT for 9 weeks under continuous agitation. EDTA was refreshed weekly, and every two weeks, samples were placed in 10% buffered formaldehyde for 48 h to maintain formalin tissue fixation. Sections (5 μm thick) were stained with hematoxylin and eosin and with Picrosirus red/ Alcian blue staining protocols [33] and evaluated in a blind and random order by two investigators (AT, IR) using the histological grading system validated for use in dogs [34] using an Olympus BX41 microscope. To detect changes in collagen deposition, immunohistochemistry for collagen type I, II and X was performed. To explore the disease modifying role of celecoxib, the immunopositivity of NGF, a well-known angiogenic and neurotrophic factor [8], was assessed by counting the percentage of immunopositively stained cells over total number of cells in the NP and ventral and dorsal AF. Specifications of the antigen retrieval and respective antibody concentrations are given in supplementary file 2. Briefly, deparaffinization was established through xylene (2 × 5 min) and graded ethanol (96, 80, 70, 60% *v*/v, 5 min each), followed by two rinses of TBS + 0.1% v/v Tween (TBST0.1%, 2 × 5 min). Antigen retrieval was performed, followed by endogenous peroxidase inhibition for collagen I, II and X for 5 min and pre-incubation with blocking buffer for 30 min at RT. Thereafter, sections were incubated with primary antibody at 4 °C overnight (Collagen I, II, and X) or 3 h at RT for NGF. The EnVision-HRP detection system (Dako) was applied for 30 min at RT followed by incubation with streptavidin conjugated with horseradish peroxidase for 30 min at RT. All antibodies were visualized with the liquid DAB+ substrate chromogen (Dako). All stainings were accompanied by appropriate positive and negative (isotype) controls. Negative control did not show positive immunostaining.

2.4.5. GAG, DNA, collagen and PGE_2 content of the nucleus pulposus and annulus fibrosus

Transverse cryosections (60 μm thick) of the snap frozen IVDs were collected on glass slides. Immediately thereafter, the NP and AF were separated and collected in 400 μL and 750 μL cOmplete lysis M EDTA-free buffer (Roche Diagnostics Nederland BV), respectively and stored at −80 °C until analysis. For biochemical analyses, the NP and AF were homogenized in cOmplete lysis M EDTA-free buffer in a TissueLyser II (Qiagen) for 2 × 30 seconds at 20 Hz. Inhibition of COX-2 activity was determined by measuring PGE_2 levels in the supernatants by ELISA as mentioned previously. The supernatant and pellet of each NP and AF sample was digested overnight in papain buffer (250 μg/mL papain (P3125, 100 mg, Sigma-Aldrich) and 1.57 mg/mL cysteine HCl (C7880, Sigma-Aldrich). The 1,9-dimethylmethylene blue (DMMB) assay was used to quantify glycosaminoglycan (GAG) content [35] of the pellets and supernatants. GAG concentrations were calculated by using chondroitin sulphate from shark cartilage (C4384, Sigma-Aldrich) as a standard and the absorbance was read at 540/595 nm. The Quant-iT™ dsDNA Broad-Range assay kit in combination with a Qubit™ fluorometer (Invitrogen) was used in accordance with the manufacturer's instructions to determine the DNA content of the papain-digested NP and AF pellets. Collagen content was quantified in the pellets of the NP and AF by using a hydroxyproline assay according to the method of Neuman and Logan [36]. Papain digested samples were freeze-dried overnight, hydrolysed at 108 °C overnight in 4 M NaOH, centrifuged (15 s at 14,000 g) and stored at −20 °C. Prior to measurements, samples were centrifuged (15 s at 14,000 g) once more, chloramine T reagent (2426, Merck, Schiphol-Rijk, The Netherlands) was added, and samples were allowed to shake for 20 min at 170 rpm. Freshly prepared dimethylaminobenzaldehyde (3058, Merck) was added, and samples

were incubated for 20 min at 60 °C. The absorbance was read at 570 nm and collagen content was calculated from the hydroxyproline content by multiplying with a factor 7.5 [36]. DNA and collagen content in the supernatants were negligible and therefore not included in the calculations. Total GAG, collagen and PGE_2 content were normalized to DNA content of the sample.

2.5. Statistical analysis

Statistical analysis was conducted using SPSS software, version 22.0 and R studio software v3.3.1. Normality of the data was checked by assessing the Q-Q plots, histograms and Shapiro-Wilks tests. For non-parametric distributed data, Kruskall Wallis tests and subsequently Mann Whitney *U* tests were used. For normally distributed data, a general linear model was applied employing "dog" and "IVD level" as a random effect and "treatment" as fixed effect. The Benjamini & Hochberg test was used to correct for multiple testing. For categorical data, the *Monte-Carlo* re-sampling bootstrapping method was used. A two-sided Mann-Whitney Wilcoxon test was performed for an independence test of categorical data, using R studio software (*RStudio* v3.3.1). *P* values < .05 were considered as statistically significant after correction for multiple testing.

Effect sizes (ES) were retrieved as *Hedge's g* for parametric data*:* medium, 0.5–0.8; large, 0.8–1.2; 1.2–2, very large and > 2 huge [37]. Differences were considered as relevant when $p < .05$ and/or ES was medium or larger when *p*-value was < 0.1. For non-parametric data, Cliff's delta was assessed: $0.28 < ES < 0.43$, medium; $0.43 \leq ES < 0.7$, large; $ES \geq 0.7$, extra-large [38].

3. Results

3.1. In vitro celecoxib release

3.1.1. Microsphere characterization

The obtained PEA polymer had an average molecular weight (Mn) of 70 kDa and a polydispersity index (PDI) of 1.70 (Table 2)(Fig. 3). The average particle size of the unloaded microspheres was 31.9 μm, whereas the CXB-loaded particles had an average diameter of 25.3 μm (Table 1). This difference in size was mainly due to the different viscosity of the used oil phase with respect to polymer:solvent ratio, since for the preparation of CXB-loaded PEAMs a 5% (wt/v) ratio was used compared to 15% (wt/v) for unloaded microspheres.

3.1.2. Celecoxib was gradually released from polyesteramide microspheres for 28 days

Celecoxib release was determined in PBS for 14 days (Fig. 2B,C) and in the presence of cultured NP cells provided with a pro-inflammatory stimulus for 28 days (Fig. 2D). In both experiments, there was a gradual release of CXB from the PEA microspheres (Fig. 2D). After 14 and 28 days, 30% and 40%, respectively, of the CXB was released from the PEA microspheres. The released CXB from the PEAMs, corresponding with 10^{-7} M, was close to the lower detection limit of the ELISA and was almost undetectable after 28 days of release. As such, the cumulative release of CXB from the low dose PEAM-condition was most probably underestimated and accounted for ~20%.

Table 2
Polymer characterization.

	Mn (kDa)	PDI	Tg	Relative monomer ratio
PEA III Ac Bz	69.5	1.70	54.3 °C	0.30:0.27:0.43

The relative ratio between the polymer building blocks was determined by Nuclear Magnetic Resonance (^{1}H NMR). Glass-liquid transition temperature (Tg) of the polymer was determined under dry conditions by differential scanning calorimetry (DSC). Mn, number of average molecular weight; PDI, polydispersity index.

3.1.3. PEA based celecoxib-loaded microspheres exerted an anti-inflammatory and possibly anti-catabolic effect on canine nucleus pulposus cells from degenerated IVDs

The 10^{-6} M CXB-"bolus" and the 10^{-4} M CXB-PEAMs were both able to significantly suppress PGE_2 production in NP cells during the entire 28 days culture period (Fig. 4A, $p = .0001$ and $p = .003$, respectively). Even on day 28, PGE_2 production was inhibited by 80% and 78% (Fig. 4B) by CXB-bolus ($p = .003$) and released from 10^{-4} M CXB-PEAMs ($p < .0001$), respectively. The CXB released from the 10^{-7} M CXB-PEAMs was not able to effectively inhibit PGE_2 production demonstrating dose-dependent bioactivity of the released CXB. In line with this thought, CXB levels released by the 10^{-7} M CXB-PEAMs during the 1st day of culture were ~20 lower than those measured in the 10^{-6} M CXB-bolus group. There were no differences in total DNA content between conditions at any of the time points, indicating no effect of CXB-PEAMs on the cumulative result of proliferation and/or cell death regardless of the loading dose.

On day 4, RT-qPCR analysis of NP cells from degenerated IVDs revealed a downregulation of *MMP13* mRNA expression in the 10^{-4} M CXB-PEAMs group compared to the control and CXB-bolus group (Fig. 4C, $p = .074$, large ES; $p = .03$ respectively). mRNA levels of *ADAMTS5* (Fig. 4D) and *TIMP1* (data not shown) were not influenced by CXB-loaded PEAMs. *COL2α1* mRNA expression was increased in both CXB-PEAM groups compared to the control and CXB-bolus group (Fig. 4E, $p = .005$, $p = .007$, respectively). *ACAN* mRNA expression tended to be higher in the 10^{-7} M CXB-PEAMs *vs.* control group ($p = .07$; very large ES). Expression of *COL1α1* between conditions (Fig. 4G) was not affected. The mRNA expression of the pro-apoptotic gene *CASP3* was lowered by 10^{-4} M CXB-PEAMs ($p = .06$, huge ES) *vs.* control, while the mRNA expression and ratio of pro-apoptotic (*BAX*) and anti-apoptotic (*BCL2*) markers were not affected by the culture conditions. The expression of proliferative markers *CCDN1* and *AXIN2* were not influenced by any of the culture conditions (data not shown), in line with the DNA measurements.

3.2. In vivo induced IVD degeneration

3.2.1. Magnetic resonance imaging revealed a protective effect of controlled release of celecoxib on T2 relaxation time and disc height index

All dogs showed uneventful recovery from induction surgery and were ambulant the next day. One dog appeared to have 8 lumbar vertebrae; therefore the total number of spinal units analysed was 43 instead of 42. One dog showed minor reductions in spinal reflexes of the left hind limb related to the surgical approach that recovered within 7 days. Four weeks after induction of IVD degeneration, there was a significant decrease ($p < .01$) in T2 relaxation times, which remained low at 12 weeks follow-up with concurrent increase in the Pfirrmann grade and decrease in T1ρ relaxation times (both $p < .05$) (Fig. 5A-C). In line with these findings, the DHI was unchanged at 4 weeks after induction, but tended to be decreased at 12 weeks follow-up (Fig. 5D; $p = .06$; medium ES). The sustained release of CXB resulted in minor improvement of Pfirrmann grade (only for HD-CXB-PEAMs with $p = .08$; large ES) and T2 relaxation times 12 weeks after injection, more pronounced in the HD-CXB-PEAM than in the LD-CXB-PEAM group ($p = .03$, $p = .07$; medium ES, respectively). While T1ρ relaxation times remained unchanged, intradiscal application of LD-PEAM and HD-PEAM CXB demonstrated minor improvement on DHI ($p = .06$; $p = .07$; both medium ES respectively) 12 weeks after injection.

3.2.2. Computed tomography showed no adverse effects 12 weeks after treatment

Adverse effects after local delivery of CXB-loaded PEAMs were not detected on MRI and CT. In 2/6 degenerated control IVDs, sclerosis of both end plates was visible and in 1/6 levels, early spondylosis

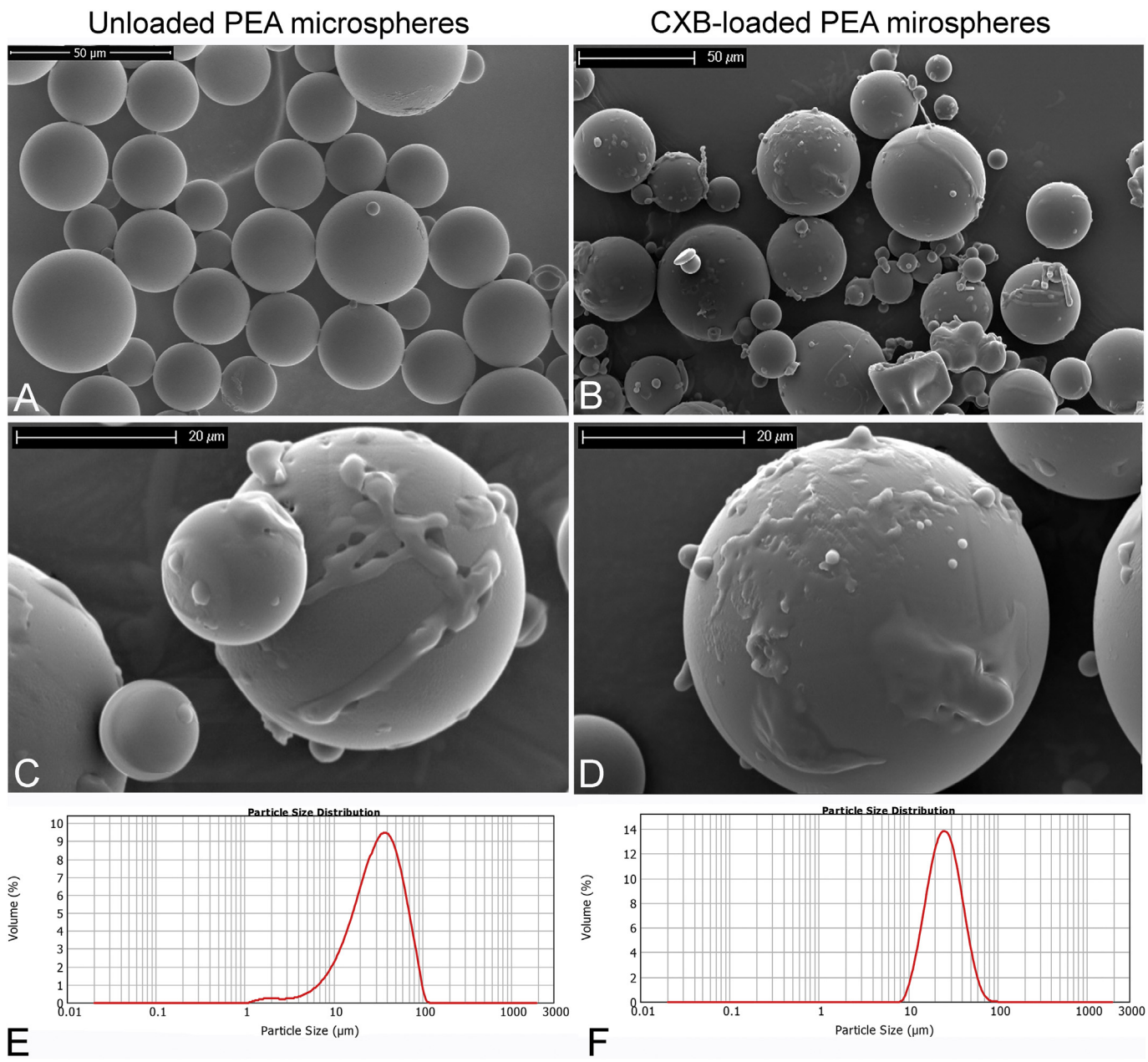

Fig. 3. Scanning electron microscopy pictures (SEM) of unloaded (A, C) and celecoxib-loaded (B, D) polyesteramide microspheres, with concurrent particle size distributions (E, F).

deformans was present at the caudal vertebral body. In the discs treated with the LD-CXB-PEAMs, there was early spondylosis formation present on the caudal vertebral body of 1 spinal unit (1/6), and subtle sclerosis of both end plates in another spinal unit (1/6). No abnormalities were noted in the discs treated with the HD-CXB-PEAMs or the other, non-induced levels. Sclerosis and spondylosis were mostly prominent on the left side where induction of disc degeneration was performed.

3.2.3. Macroscopic and microscopic evaluation of the IVDs showed a beneficial effect of celecoxib-PEAMs on macroscopic scoring of IVD degeneration

Post-mortem, macroscopic degeneration scores according to the Thompson scale were assigned to 55 IVDs (Fig. 6). The median Thompson score for the control degenerated discs was 3, which was significantly higher ($p = .017$) than the score for the non-induced discs (median 2). The degenerated discs that were injected with CXB-loaded PEAMs did not statistically differ from the non-induced or the control degenerated discs.

Histological scores ranged from 3 to 13 (Fig. 6), corresponding with slight to moderate degeneration (as the histological score ranges from 0 to 29). The overall histological scores in the degenerated discs treated with the unloaded PEAMs where higher than the non-induced discs and discs treated with the LD- and HD-CXB-PEAM ($p = .004$; $p = .04$; $p = .02$, respectively). Interestingly, the amount of subchondral sclerosis and new bone formation on the ventral aspect of the vertebrae was increased in induced (control) degenerated discs ($p < .01$, Fig. 6), but not in IVDs treated with CXB-loaded PEAMs. There were no differences in collagen type I or collagen type II deposition between the treatment groups. Collagen type X was absent in all of the investigated IVDs, while its presence was confirmed in positive controls (*i.e.* hypertrophic zone of a canine growth plate). The induction of IVD degeneration led to the increased immunopositivity of NGF in the NP (Fig. 6, $p < .001$), dorsal (Fig. 6, $p < .001$) and ventral AF ($p < .001$, data not shown), which was effectively decreased by both the low

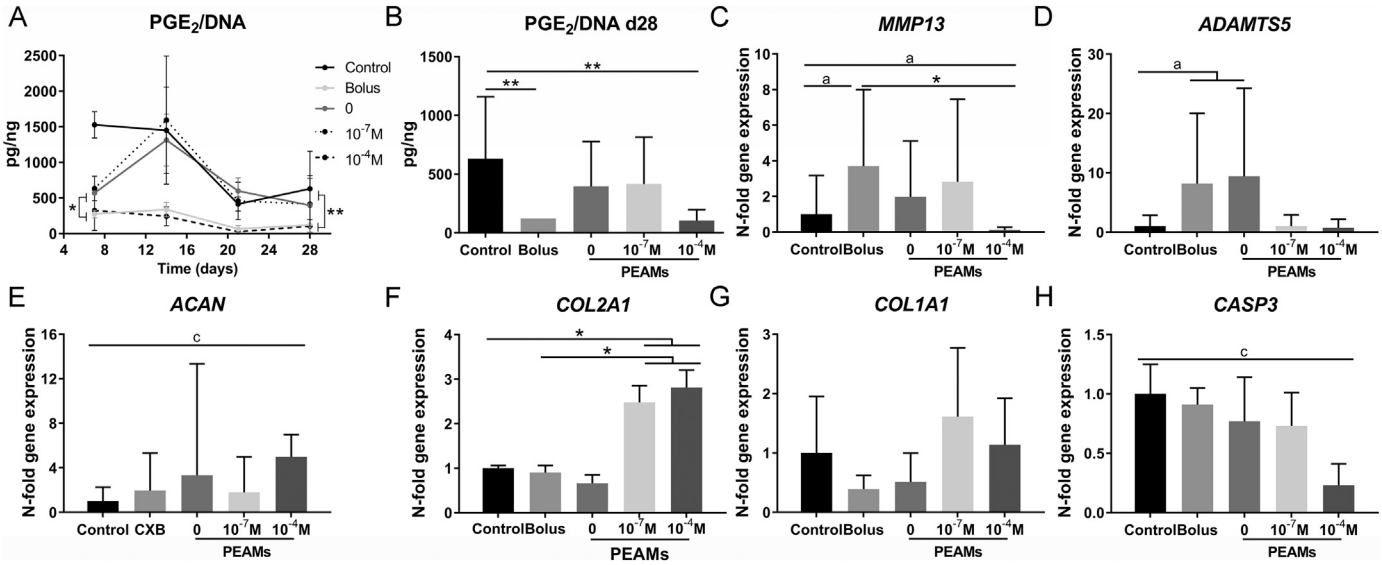

Fig. 4. Controlled release of celecoxib (CXB) is able to inhibit prostaglandin E_2 (PGE_2) production over a prolonged period of time and exerts an anabolic and anti-catabolic effect. Nucleus pulposus cells isolated from early degenerated canine intervertebral discs were subjected to a pro-inflammatory stimulus (10 ng/mL TNFα) in the presence of unloaded polyesteramide microspheres (0 PEAMs), and microspheres loaded with 10^{-7} M CXB and 10^{-4} M CXB, or CXB bolus at 10^{-6} M. PGE_2/DNA during the entire culture period (A) and PGE_2/DNA at day 28 of culturing (B). Relative *MMP13* (C), *ADAMTS5,* (D), *COL2A1* (E), *ACAN* (F), *COL1A1* (G) and *CASP3* (H) expression at $t = 4$ days. Control (chondrogenic medium with 10 ng/mL TNF-α) values were set at 1. * $p < .05$; a, medium ES; c, very large ES. $n = 6$ donors per condition and time point, in technical duplicates.

($p < .001$, $p = .026$ and $p = .004$ for the NP, ventral and dorsal AF, respectively) and the high dose ($p < .001$, $p = .002$ and $p = .003$ for the NP, ventral and dorsal AF, respectively) CXB-loaded microspheres.

3.2.4. Controlled release of celecoxib resulted in decreased PGE_2 levels and prevented GAG loss

Induction of IVD degeneration led to increased total PGE_2 tissue levels in both the NP and AF ($p = .03$, $p = .008$, Fig. 7a). Celecoxib released from LD-CXB-PEAMs and HD-CXB-PEAMs reduced the PGE_2/DNA levels in the NP with 52% and 73% respectively ($p = .09$ and $p = .068$; ES 0.49 and 0.50). This resulted in a borderline significantly lower PGE_2/DNA (Fig. 7A; $p = .054$; $p = .052$; medium ES) compared to control degenerated tissues. In the AF, PGE_2/DNA (Fig. 6B) tended to be higher in the control degenerated IVDs compared to the non-induced discs ($p = .06$; ES 1.0) and HD-CXB-PEAMs ($p = .089$; large ES). Also in the AF, PGE_2 production was 63% and 76% suppressed by the LD- and HD-CXB-PEAMs respectively ($p = .007$ and $p = .003$). In the NP, the total GAG content and the GAG content corrected for DNA (Fig. 7C) were significantly lower in degenerated control IVDs compared to non-induced discs and both CXB-PEAM groups ($p < .05$), while the latter two did not differ from the non-induced IVDs. In the AF, the GAG/DNA levels were not affected by the application of any treatment (Fig. 7D).

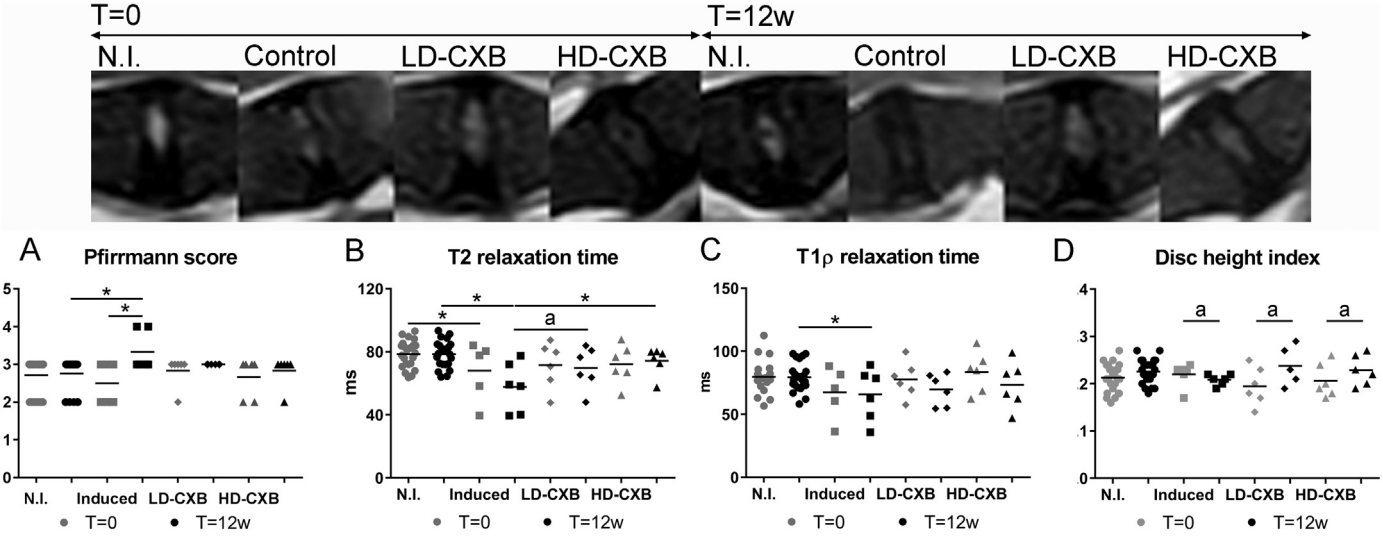

Fig. 5. Effect of *in vivo* induction of intervertebral disc (IVD) degeneration and its treatment with celecoxib (CXB)-loaded polyesteramide microspheres (PEAMs) on magnetic resonance imaging parameters. T2 relaxation times (B) were significantly decreased four weeks after IVD degeneration induction surgery (grey markers, $T = 0$). In degenerated IVDs that received unloaded PEAMs (control) compared to non-induced healthy IVDs (N.I.), Pfirrmann score (A) was increased, T2 relaxation times (B) and T1ρ relaxation times (C) were decreased at 12 weeks (black markers) and disc height index (DHI) tended to decrease with a medium ES. T2 relaxation times of IVDs treated with HD-CXB-PEAMs were significantly higher than control IVDs. The disc height index (D; DHI) was maintained (tended to improve with large ES) in the IVDs treated with either LD- or HD-CXB-PEAMs. $n = 6$ IVDs per group ($n = 24$ for the non-induced IVDs).* $p < .05$; a, medium effect size. Horizontal bar indicates median (categorical data) or mean (continuous data).

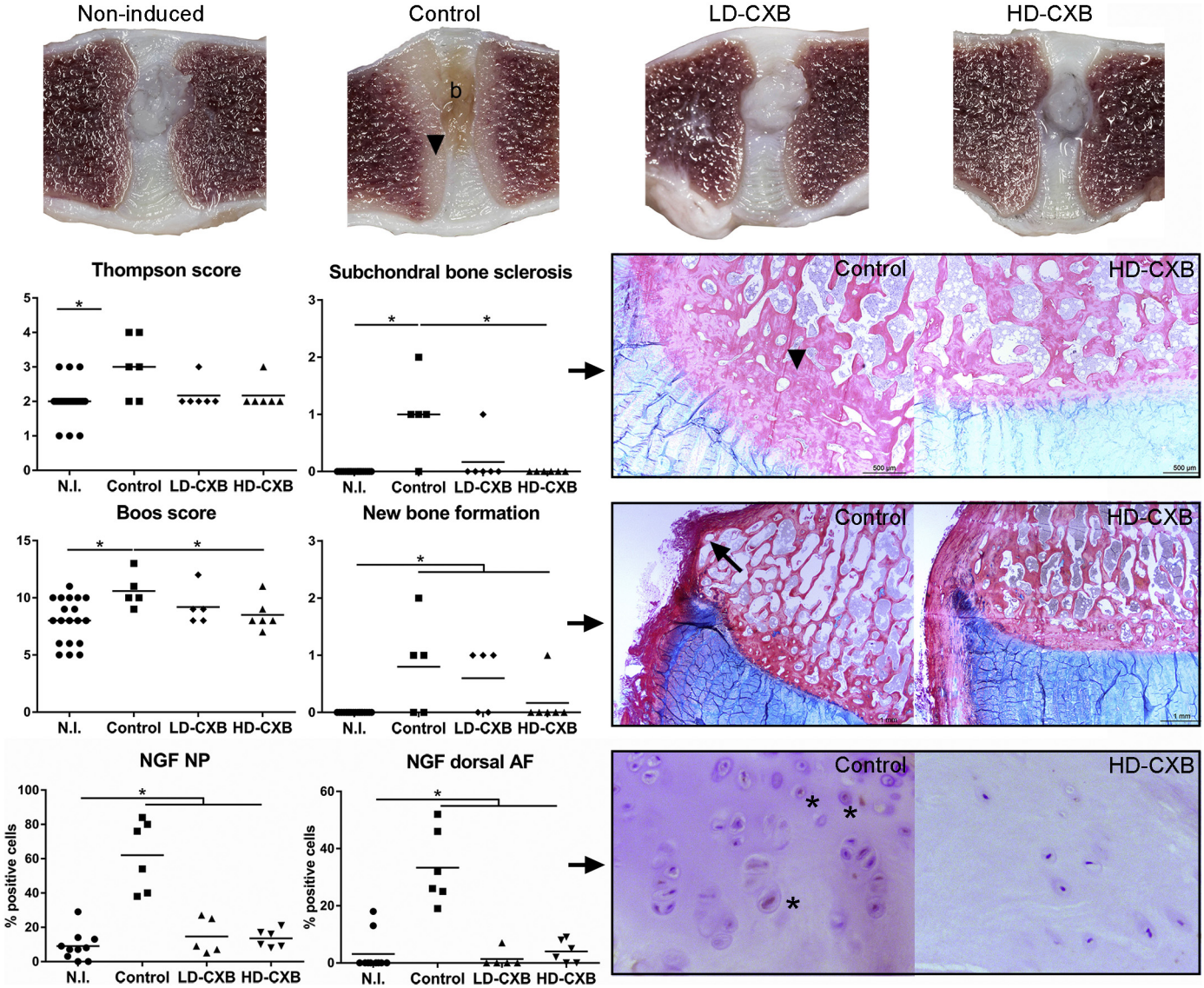

Fig. 6. Controlled release of celecoxib (CXB) inhibited progression of intervertebral disc degeneration (IVDD), the development of subchondral bone sclerosis and osteophyte formation, and the immunopositivity of nerve growth factor (NGF). Representative macroscopic images of non-induced (N.I.), degenerated control, low dose (LD) CXB and high dose (HD) CXB IVDs, with the associated macroscopic (Thompson) degeneration score, showing less degeneration in discs treated with the CXB-loaded polyesteramide microspheres (PEAMs). Note the brown discoloration (b) in the induced IVDs which is absent on all CXB-treated IVDs. Controlled release of 280 µg/ 40 µL CXB-loaded PEAMs (HD-CXB-PEAM) resulted in less severe degeneration at the histologic level (overall Boos score). Detailed analysis of sub-scores of the Boos scores revealed less subchondral bone sclerosis and less new bone formation (black arrow). The arrowhead illustrates a typical example of subchondral bone sclerosis. Increased nerve growth factor (NGF) expression (* indicate immunopositive cell within the nucleus pulposus (NP)) was observed in degenerated control IVDs (both NP and annulus fibrosus (AF)), but not in IVDs treated with CXB-PEAMs. *$p < .05$. $n = 6$ IVDs per PEAM group; $n = 24$ non-induced IVDs. (For interpretation of the references to colour in this figure legend, the reader is referred to the web version of this article.)

There seemed to be a decrease in total collagen content in the NP as a result of IVDD induction (Fig. 7E; $p = .036$). DNA content of the AF increased due to IVDD induction (Fig. 7H; $p = .051$, very large ES), but DNA content remained unchanged in the NP (Fig. 7G).

4. Discussion

This study demonstrated that sustained release of celecoxib from PEA microspheres was able to (1) suppress in a sustained manner PGE_2 production *in vitro* and *in vivo* and (2) counteract the detrimental effects of induced degeneration *in vivo* in a canine model of IVD degeneration. Intradiscal treatment with celecoxib-loaded PEA microspheres, resulting into an intradiscal dose of 280 µg, maintained T2 relaxation times on MRI and GAG content on biochemical level, improved the overall histological score of IVDs and inhibited early subchondral bone changes.

The polymer applied was based on α-amino acids, aliphatic dicarboxylic acids and aliphatic α-ω diols. The polymer has been built of three di-amino monomers connected with di-acid like in a polycondensation reaction. The monomers were chosen to balance mechanical and barrier properties of the biomaterial, controlling hard to soft segment ratio. Furthermore, these polymers showed remarkable shelf life time and could be easy processed to variety of forms such as the injectable particles described in this paper. The synthesis of PEA yielded a random *co*-polymer of high molecular weight (typically above 70 kDa). This resulted in a very good consistency of the material barrier properties when derived from different batches.

Release of celecoxib from PEAMs was shown for at least 28 days *in vitro* and suppressed PGE_2 production in TNF-α-stimulated NP cells from degenerated canine IVDs during the entire culture period, without

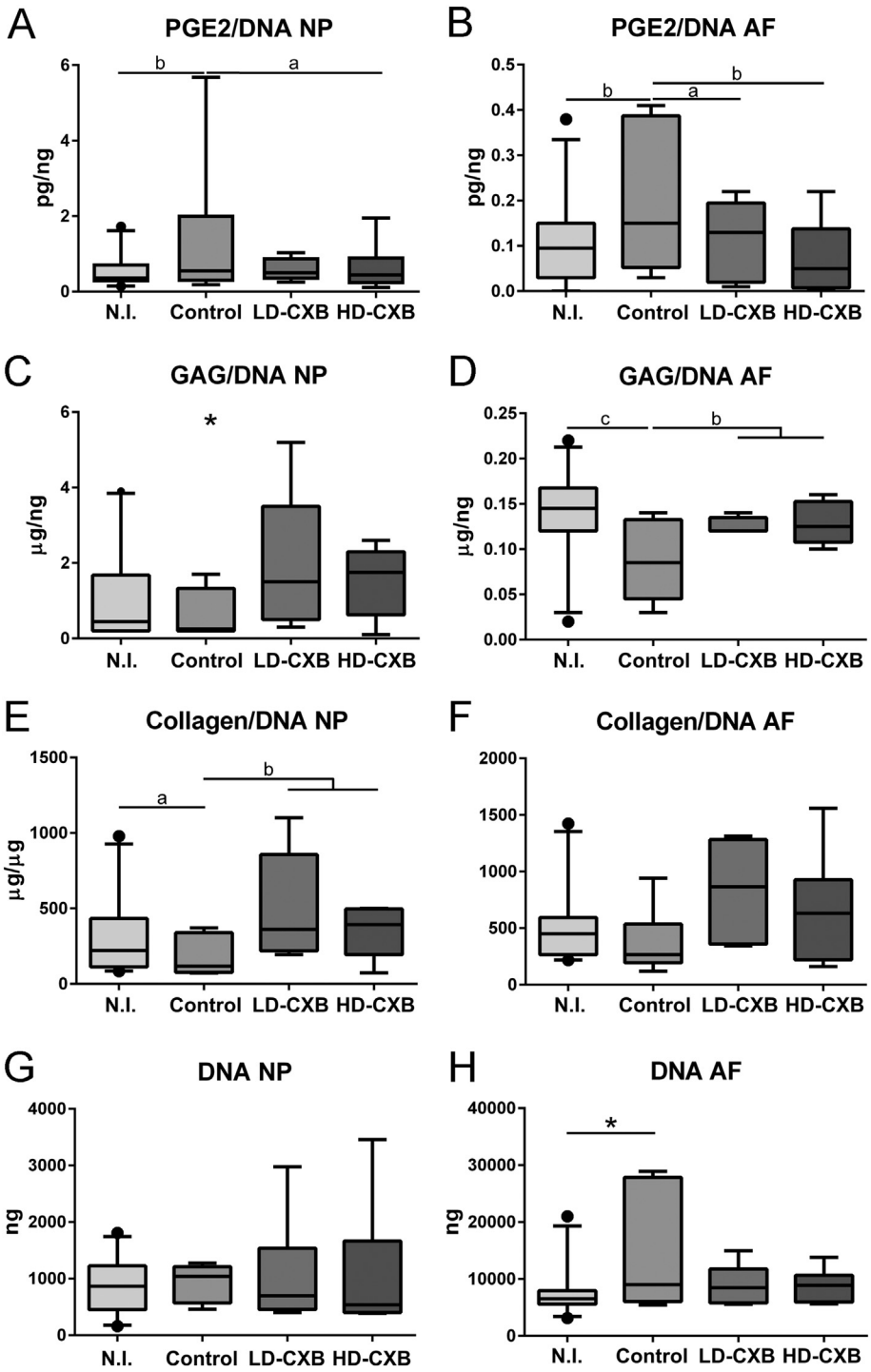

Fig. 7. Celecoxib (CXB)-loaded microspheres inhibited prostaglandin E_2 (PGE_2) production and maintained glycosaminoglycan (GAG) content in comparison to control degenerated intervertebral discs (IVDs). PGE_2/DNA (A,B), GAG/DNA (C,D), Collagen/DNA (E,F) and total DNA (G,H) of the nucleus pulposus (NP) and annulus fibrosus (AF) with indicated mean values ± SD. * $p < .05$; a, medium ES; b, large ES; c, very large ES (> 1.2). $n = 6$ IVDs per group, $n = 24$ for the non-induced IVDs (N.I.) group. N.I., non-induced; control, degenerated discs receiving unloaded microspheres; LD, low dose (1.05 mg/mL) CXB-loaded microspheres; HD, high dose (35 mg/mL) CXB-loaded microspheres.

affecting DNA content. Moreover, the mRNA expression of matrix degrading enzymes (*MMP13* and *ADAMTS5*) was inhibited and *COL2aI* and *ACAN* were enhanced. Controlled release of celecoxib with corresponding PGE_2 inhibition was previously shown for celecoxib released from PLGA microspheres in human chondrocytes from degenerated cartilage: sustained celecoxib release was confirmed for over 100 days and PGE_2 inhibition for 21 days [39]. PLGA microspheres disintegration resulted in acidic end products, which could induce toxic local pH levels [40, 41]. The more novel PEA platform does not result in toxic degradation products [26]. Extended release of celecoxib from PEA microspheres has been demonstrated in PBS; after 80 days, almost 50% was released into the medium. In the same study, the release of small molecules from PEA microspheres has shown to be accelerated through serine proteases from neutrophil cell lysate [22], indicating a possible a discrepancy between *in vitro* and *in vivo* release. However, the *in vitro* release of celecoxib in the present study seemed not to be overtly influenced by the presence of NP cells stimulated with TNF-α. Considering that *in vivo*, even chronically degenerated IVDs do not contain an abundance of (inflammatory) cells and inflammation is usually low-grade [42], when compared to neutrophil like cell lysate, celecoxib release from PEAMs might also be more gradual in the degenerated disc environment.

The applicability of celecoxib delivery in harnessing tissue inflammation and pain-parameters was also confirmed *in vivo* in a large

animal model with experimentally induced IVD degeneration. In this study, PGE_2 production associated with the induction of IVD degeneration was inhibited up to 53% and 73% on average by a loading dose of 8.4 μg and 280 μg celecoxib, respectively. In a previous study, sustained local delivery of 10^{-5} M celecoxib in a pNIPAAM-based hydrogel in a canine model with spontaneous early IVD degeneration resulted in a maximal PGE_2 decrease of 35% [27]. This indicates that with increasing celecoxib loading dosages, there is more PGE_2 suppression. However, both in the spontaneous as in the induced degeneration canine models, the degeneration score was mild to moderate, but without overt clinical signs. Although enhanced PGE_2 production is known to increase with advancing degeneration, the most dramatic increase takes place when extrusion or protrusion of the IVD is present [42]. Because in both animal models, degeneration of the IVDs was not accompanied by protrusion or extrusion of IVD tissue, nor clinical signs indicating symptomatic IVD disease, PGE_2 levels were probably lower than in symptomatic IVDs as suggested earlier by retrospective analysis of symptomatic *vs* asymptomatic degenerated NP tissues [42]. A larger effect on PGE_2 levels could therefore be expected in symptomatic IVDs. In line with this thought, in canine patients suffering from spontaneous IVDD with low back pain, local injection of a controlled-release platform loaded with celecoxib corresponding with 10^{-5} M at the NP level resulted in a decrease of clinical signs for up to two months [43]. In addition to a decrease in PGE_2 levels, in the present study the controlled release of celecoxib also resulted in a decrease in NGF expression. NGF not only stimulates development of sensory nerve endings in degenerating IVDs, it can also generate pain by directly influence nerve fibers to produce nociceptive neuropeptides and express receptors that are associated with inflammatory pain, and has been known to induce matrix degrading enzymes [8]. Altogether, reduction of local PGE_2 levels and NFG immunopositivity were effectuated after local delivery of the celecoxib-loaded PEAMs indicating promising disease-modifying effects of this platform for chronic back pain related to IVD degeneration.

Interestingly, intradiscal application of celecoxib-loaded PEAMs prevented GAG loss in the degenerating NP indicative of structural repair. On MRI, induction of degeneration resulted in a decrease in signal intensity and T2 values indicating loss of proteoglycans and water, and thus advancing degeneration, which was confirmed by histology and biochemistry. Local application of HD-CXB-PEAMs reversed the degenerative process within the NP, where higher T2 values were detected, indicating preserved water content and integrity of collagen fibers. Accordingly, on biochemical level, there also appeared to be an improved GAG/DNA content and less overall collagen loss in the HD-CXB-PEAM treated IVDs. In line with these findings, in patients suffering from osteoarthritis, proteoglycan synthesis rate and retention of newly formed proteoglycans were significantly increased after oral celecoxib treatment compared to controls [44, 45], suggesting celecoxib as a disease-modifying drug. The mechanism of action of locally delivered celecoxib-loaded PEAMs could be dual: by harnessing inflammation and thereby limiting the amount of pain mediators and/or by inhibiting proteoglycan degradation. Both are mechanisms that inhibit ingrowth of neural and vascular tissue [8, 46].

Another source of back pain could be the subchondral endplate. Subchondral vertebral bone changes are common in chronic IVDD [3] and are referred to as Modic changes (MC) on MRI [47]. All types of MC are associated with chronic low back pain and worse disease outcome [48]. They are interconvertible and most probably reflect different disease stages [49]. The present study demonstrated a low frequency of MC, most probably related to the relatively short term follow up (*i.e.* 12 weeks after induction), which was only present in degenerated untreated discs allowing for no concrete conclusions. However, histological analysis revealed that the controlled release of celecoxib was able to prevent early subchondral bone changes, *i.e.* subchondral vertebral sclerosis and early new bone formation on the ventral vertebral margins. Interestingly, subchondral bone pathology in IVD degeneration shows striking similarities to subchondral bone remodeling in osteoarthritis and its relation to joint pain [50, 51]. In OA, the effect of celecoxib on subchondral bone has been studied in more detail [52], as subchondral bone sclerosis and osteophytes are hallmarks of degenerative joint disease [53, 54]. A daily oral dose of CXB significantly reduced osteophyte formation in a rat model of osteoarthritis [45], which was also seen after intra-articular injection of CXB in PEA microspheres in a preclinical OA rat model [55]. As such, it is tempting to hypothesize that local sustained delivery of a COX-2 inhibitor not only improves structural integrity of the NP itself, it also has the potency to improve subchondral bone health benefiting thereby the affected spinal segment.

To conclude, the *in vitro* and *in vivo* results indicate that controlled release platforms based on PEA microspheres seem very promising for therapeutic application for chronic back pain related to IVD degeneration. Celecoxib incorporated in PEAMs was safely administered intradiscally in experimental dogs, and exerted anti-inflammatory and anti-degenerative effects. These findings imply that local sustained presence of celecoxib may have the ability to harness inflammation and by reducing pain mediators, such as PGE_2 and NGF, may also result into less pain in a clinical setting. Follow-up studies focusing on pain and on a better understanding of how particle degradation and inherent drug release kinetics are influenced by the disease-state of the tissue are warranted to determine the efficacy of celecoxib-loaded PEAMs in inhibiting low back pain.

Author contributions

Conception and design: MT, BM, LC and AT. Collection and assembly of data: AT, MT, FCB, MB, IR. Statistical expertise: AT, AMB. Drafting of the article: AT. Revising manuscript content: all authors.

Role of the funding source

Financial support was granted by LSH Ariadne and the Dutch Arthritis Foundation (LLP22 and LLP12) and is greatly acknowledged.

Conflict of interest

The authors from DSM have proprietary and commercial interest in material discussed in this article. All other authors: none.

Acknowledgements

The authors would also like to thank Harry van Engelen, Saskia Plomp and Simone Kamphuijs for their assistance with data acquisition the *in vivo* experiment.

Appendix A. Supplementary data

Supplementary data to this article can be found online at https://doi.org/10.1016/j.jconrel.2018.08.019.

References

[1] D. Hoy, L. March, P. Brooks, F. Blyth, A. Woolf, C. Bain, G. Williams, E. Smith, T. Vos, J. Barendregt, C. Murray, R. Burstein, R. Buchbinder, The global burden of low back pain: estimates from the global burden of disease 2010 study, Ann. Rheum. Dis. 73 (2014) 968–974.
[2] W. Kaplan, V. Wirtz, A. Mantel-Teeuwisse, P. Stolk, B. Duthey, R. Laing, Priority Diseases and Reasons For Inclusion, Priority Medicines for Europa and the World. 2013 Update, (2013), pp. 165–168.
[3] E.I. de Schepper, J. Damen, J.B. van Meurs, A.Z. Ginai, M. Popham, A. Hofman, B.W. Koes, S.M. Bierma-Zeinstra, The association between lumbar disc degeneration and low back pain: the influence of age, gender, and individual radiographic features, Spine (Phila Pa. 1976), 35 (2010), pp. 531–536.
[4] M.C. Battie, T. Videman, J. Kaprio, L.E. Gibbons, K. Gill, H. Manninen, J. Saarela, L. Peltonen, The twin spine study: contributions to a changing view of disc degeneration, Spine J. 9 (2009) 47–59.

[5] M.V. Risbud, I.M. Shapiro, Role of cytokines in intervertebral disc degeneration: pain and disc content, Nat. Rev. Rheumatol. 10 (2014) 44–56.
[6] M.A. Adams, P.J. Roughley, What is Intervertebral Disc Degeneration, And What Causes It? Spine (Phila Pa. 1976), 31 (2006), pp. 2151–2161.
[7] A.J. Freemont, The cellular pathobiology of the degenerate intervertebral disc and discogenic back pain, Rheumatology (Oxford) 48 (2009) 5–10.
[8] S.E. Navone, G. Marfia, A. Giannoni, M. Beretta, L. Guarnaccia, R. Gualtierotti, D. Nicoli, P. Rampini, R. Campanella, Inflammatory mediators and signalling pathways controlling intervertebral disc degeneration, Histol. Histopathol. 32 (2017) 523–542.
[9] B.A. Walter, D. Purmessur, M. Likhitpanichkul, A. Weinberg, S.K. Cho, S.A. Qureshi, A.C. Hecht, J.C. Iatridis, Inflammatory kinetics and efficacy of anti-inflammatory treatments on human nucleus pulposus cells, Spine (Phila Pa. 1976) 40 (2015) 955–963.
[10] H. Miyamoto, M. Doita, K. Nishida, T. Yamamoto, M. Sumi, M. Kurosaka, Effects of cyclic mechanical stress on the production of inflammatory agents by nucleus pulposus and anulus fibrosus derived cells in vitro, Spine (Phila Pa. 1976) 31 (2006) 4–9.
[11] T.A. Samad, K.A. Moore, A. Sapirstein, S. Billet, A. Allchorne, S. Poole, J.V. Bonventre, C.J. Woolf, Interleukin-1beta-mediated induction of cox-2 in the CNS contributes to inflammatory pain hypersensitivity, Nature 410 (2001) 471–475.
[12] M. Sekiguchi, K. Otoshi, S. Kikuchi, S. Konno, Analgesic effects of prostaglandin E2 receptor subtype EP1 receptor antagonist: experimental study of application of nucleus pulposus, Spine (Phila Pa. 1976) 36 (2011) 1829–1834.
[13] J. Simon, M. McAuliffe, F. Shamim, N. Vuong, A. Tahaei, Discogenic low back pain, Phys. Med. Rehabil. Clin. N. Am. 25 (2014) 305–317.
[14] F.C. Bach, N. Willems, L.C. Penning, K. Ito, B.P. Meij, M.A. Tryfonidou, Potential regenerative treatment strategies for intervertebral disc degeneration in dogs, BMC Vet. Res. 10 (2014) (3-6148-10-3).
[15] D. Sakai, S. Grad, Advancing the cellular and molecular therapy for intervertebral disc disease, Adv. Drug Deliv. Rev. 84 (2015) 159–171.
[16] S. Motaghinasab, A. Shirazi-Adl, M. Parnianpour, J.P. Urban, Disc size markedly influences concentration profiles of intravenously administered solutes in the intervertebral disc: a computational study on glucosamine as a model solute, Eur. Spine J. 23 (2014) 715–723.
[17] L. Zhang, J.C. Wang, X.M. Feng, W.H. Cai, J.D. Yang, N. Zhang, Antibiotic penetration into rabbit nucleus pulposus with discitis, Eur. J. Orthop. Surg. Traumatol. 24 (2014) 453–458.
[18] S.M. Richardson, G. Kalamegam, P.N. Pushparaj, C. Matta, A. Memic, A. Khademhosseini, R. Mobasheri, F.L. Poletti, J.A. Hoyland, A. Mobasheri, Mesenchymal stem cells in regenerative medicine: focus on articular cartilage and intervertebral disc regeneration, Methods 99 (2016) 69–80.
[19] A. Rodriguez-Galan, L. Franco, J. Puiggali, Degradable poly(ester amide)s for biomedical applications, Polymers 3 (2011) 65–99.
[20] H. Sun, F. Meng, A.A. Dias, M. Hendriks, J. Feijen, Z. Zhong, alpha-Amino acid containing degradable polymers as functional biomaterials: rational design, synthetic pathway, and biomedical applications, Biomacromolecules 12 (2011) 1937–1955.
[21] V. Andres-Guerrero, M. Zong, E. Ramsay, B. Rojas, S. Sarkhel, B. Gallego, R. de Hoz, A.I. Ramirez, J.J. Salazar, A. Trivino, J.M. Ramirez, E.M. Del Amo, N. Cameron, B. de-Las-Heras, A. Urtti, G. Mihov, A. Dias, R. Herrero-Vanrell, Novel biodegradable polyesteramide microspheres for controlled drug delivery in Ophthalmology, J. Control. Release 211 (2015) 105–117.
[22] M. Janssen, U.T. Timur, N. Woike, T.J. Welting, G. Draaisma, M. Gijbels, L.W. van Rhijn, G. Mihov, J. Thies, P.J. Emans, Celecoxib-loaded PEA microspheres as an auto regulatory drug-delivery system after intra-articular injection, J. Control. Release 244 (2016) 30–40.
[23] C.L. Le Maitre, A. Pockert, D.J. Buttle, A.J. Freemont, J.A. Hoyland, Matrix synthesis and degradation in human intervertebral disc degeneration, Biochem. Soc. Trans. 35 (2007) 652–655.
[24] N. Willems, G. Mihov, G.C. Grinwis, M. van Dijk, D. Schumann, C. Bos, G.J. Strijkers, W.J. Dhert, B.P. Meij, L.B. Creemers, M.A. Tryfonidou, Safety of intradiscal injection and biocompatibility of polyester amide microspheres in a canine model predisposed to intervertebral disc degeneration, J Biomed Mater Res B Appl Biomater 105 (2015) 707–714.
[25] N. Bergknut, J.P. Rutges, H.J. Kranenburg, L.A. Smolders, R. Hagman, H.J. Smidt, A.S. Lagerstedt, L.C. Penning, G. Voorhout, H.A. Hazewinkel, G.C. Grinwis, L.B. Creemers, B.P. Meij, W.J. Dhert, The dog as an animal model for intervertebral disc degeneration? Spine (Phila Pa. 1976) 37 (2012) 351–358.
[26] R. Katsarava, Z. Beridze, N. Arabuli, D. Kharadze, C.C. Chu, C.Y. Won, Amino acid-based bioanalogous polymers. Synthesis, and study of regular poly(ester amide)s based on bis(α-amino acid) α, ω-alkylene diesters, and aliphatic dicarboxylic acids, J. Polym. Sci. A 37 (1999) 391–407.
[27] N. Willems, H.Y. Yang, M.L. Langelaan, A.R. Tellegen, G.C. Grinwis, H.J. Kranenburg, F.M. Riemers, S.G. Plomp, E.G. Craenmehr, W.J. Dhert, N.E. Papen-Botterhuis, B.P. Meij, L.B. Creemers, M.A. Tryfonidou, Biocompatibility and intradiscal application of a thermoreversible celecoxib-loaded poly-N-isopropylacrylamide MgFe-layered double hydroxide hydrogel in a canine model, Arthritis Res. Ther. 17 (2015) (214-015-0727-x).
[28] A. Hiyama, J. Mochida, T. Iwashina, H. Omi, T. Watanabe, K. Serigano, F. Tamura, D. Sakai, Transplantation of mesenchymal stem cells in a canine disc degeneration model, J. Orthop. Res. 26 (2008) 589–600.
[29] N. Willems, F.C. Bach, S.G. Plomp, M.H. van Rijen, J. Wolfswinkel, G.C. Grinwis, C. Bos, G.J. Strijkers, W.J. Dhert, B.P. Meij, L.B. Creemers, M.A. Tryfonidou, Intradiscal application of rhBMP-7 does not induce regeneration in a canine model of spontaneous intervertebral disc degeneration, Arthritis Res. Ther. 17 (2015) 137–151.
[30] N. Bergknut, E. Auriemma, S. Wijsman, G. Voorhout, R. Hagman, A.S. Lagerstedt, H.A. Hazewinkel, B.P. Meij, Evaluation of intervertebral disk degeneration in chondrodystrophic and nonchondrodystrophic dogs by use of Pfirrmann grading of images obtained with low-field magnetic resonance imaging, Am. J. Vet. Res. 72 (2011) 893–898.
[31] H.S. An, K. Takegami, H. Kamada, C.M. Nguyen, E.J. Thonar, K. Singh, G.B. Andersson, K. Masuda, Intradiscal administration of osteogenic protein-1 increases intervertebral disc height and proteoglycan content in the nucleus pulposus in normal adolescent rabbits, Spine (Phila Pa. 1976) 30 (2005) 25–31.
[32] N. Bergknut, G. Grinwis, E. Pickee, E. Auriemma, A.S. Lagerstedt, R. Hagman, H.A. Hazewinkel, B.P. Meij, Reliability of macroscopic grading of intervertebral disk degeneration in dogs by use of the Thompson system and comparison with low-field magnetic resonance imaging findings, Am. J. Vet. Res. 72 (2011) 899–904.
[33] H.E. Gruber, J. Ingram, E.N. Hanley Jr., An improved staining method for intervertebral disc tissue, Biotech. Histochem. 77 (2002) 81–83.
[34] N. Bergknut, B.P. Meij, R. Hagman, K.S. de Nies, J.P. Rutges, L.A. Smolders, L.B. Creemers, A.S. Lagerstedt, H.A. Hazewinkel, G.C. Grinwis, Intervertebral disc disease in dogs - part 1: a new histological grading scheme for classification of intervertebral disc degeneration in dogs, Vet. J. 195 (2013) 156–163.
[35] R.W. Farndale, C.A. Sayers, A.J. Barrett, A direct spectrophotometric microassay for sulfated glycosaminoglycans in cartilage cultures, Connect. Tissue Res. 9 (1982) 247–248.
[36] R.E. Neuman, M.A. Logan, The determination of hydroxyproline, J. Biol. Chem. 184 (1950) 299–306.
[37] S.S. Sawilowsky, New effect size rules of thumb, J. Modern Appl. Stat. Methods 8 (2009) 597–599.
[38] N. Cliff, Dominance statistics: ordinal analyses to answer ordinal questions, Psychol. Bull. 114 (1993) 494–509.
[39] H.Y. Yang, M. van Dijk, R. Licht, M. Beekhuizen, M. van Rijen, M.K. Janstal, F.C. Oner, W.J. Dhert, D. Schumann, L.B. Creemers, Applicability of a newly developed bioassay for determining bioactivity of anti-inflammatory compounds in release studies–celecoxib and triamcinolone acetonide released from novel PLGA-based microspheres, Pharm. Res. 32 (2015) 680–690.
[40] T.E. Kavanaugh, T.A. Werfel, H. Cho, K.A. Hasty, C.L. Duvall, Particle-based technologies for osteoarthritis detection and therapy, Drug Deliv. Transl. Res. 6 (2016) 132–147.
[41] T. Parumasivam, S.S. Leung, D.H. Quan, J.A. Triccas, W.J. Britton, H.K. Chan, Rifapentine-loaded PLGA microparticles for tuberculosis inhaled therapy: preparation and in vitro aerosol characterization, Eur. J. Pharm. Sci. 88 (2016) 1–11.
[42] N. Willems, A.R. Tellegen, N. Bergknut, L.B. Creemers, J. Wolfswinkel, C. Freudigmann, K. Benz, G.C. Grinwis, M.A. Tryfonidou, B.P. Meij, Inflammatory profiles in canine intervertebral disc degeneration, BMC Vet. Res. 12 (2016).
[43] A.R. Tellegen, N. Willems, M. Beukers, G.C.M. Grinwis, S.G.M. Plomp, C. Bos, M. van Dijk, M. de Leeuw, L.B. Creemers, M.A. Tryfonidou, B.P. Meij, Intradiscal application of a PCLA-PEG-PCLA hydrogel loaded with celecoxib for the treatment of back pain in canines: What's in it for humans? J. Tissue Eng. Regen. Med. 12 (2018) 642–652.
[44] T.N. de Boer, A.M. Huisman, A.A. Polak, A.G. Niehoff, A.C. van Rinsum, D. Saris, J.W. Bijlsma, F.J. Lafeber, S.C. Mastbergen, The chondroprotective effect of selective COX-2 inhibition in osteoarthritis: ex vivo evaluation of human cartilage tissue after in vivo treatment, Osteoarthr. Cartil. 17 (2009) 482–488.
[45] A. Panahifar, J.L. Jaremko, A.G. Tessier, R.G. Lambert, W.P. Maksymowych, B.G. Fallone, M.R. Doschak, Development and reliability of a multi-modality scoring system for evaluation of disease progression in pre-clinical models of osteoarthritis: celecoxib may possess disease-modifying properties, Osteoarthr. Cartil. 22 (2014) 1639–1650.
[46] D. Purmessur, M.C. Cornejo, S.K. Cho, P.J. Roughley, R.J. Linhardt, A.C. Hecht, J.C. Iatridis, Intact glycosaminoglycans from intervertebral disc-derived notochordal cell-conditioned media inhibit neurite growth while maintaining neuronal cell viability, Spine J. 15 (2015) 1060–1069.
[47] M.T. Modic, J.S. Ross, Lumbar degenerative disk disease, Radiology 245 (2007) 43–61.
[48] S. Dudli, A.J. Fields, D. Samartzis, J. Karppinen, J.C. Lotz, Pathobiology of Modic changes, Eur. Spine J. 25 (2016) 3723–3734.
[49] E. Perilli, I.H. Parkinson, L.H. Truong, K.C. Chong, N.L. Fazzalari, O.L. Osti, Modic (endplate) changes in the lumbar spine: bone micro-architecture and remodelling, Eur. Spine J. 24 (2015) 1926–1934.
[50] J.P. Rutges, O.P. van der Jagt, F.C. Oner, A.J. Verbout, R.J. Castelein, J.A. Kummer, H. Weinans, L.B. Creemers, W.J. Dhert, et al., Osteoarthr. Cartil. 19 (2011) 89–95.
[51] T. Neogi, Structural correlates of pain in osteoarthritis, Clin. Exp. Rheumatol. 35 (Suppl. 107) (2017) 75–78.
[52] M.C. Zweers, T.N. de Boer, J. van Roon, J.W. Bijlsma, F.P. Lafeber, S.C. Mastbergen, Celecoxib: considerations regarding its potential disease-modifying properties in osteoarthritis, Arthritis Res. Ther. 13 (2011) 239–250.
[53] R.I. Bolbos, J. Zuo, S. Banerjee, T.M. Link, C.B. Ma, X. Li, S. Majumdar, Relationship between trabecular bone structure and articular cartilage morphology and relaxation times in early OA of the knee joint using parallel MRI at 3 T, Osteoarthr. Cartil. 16 (2008) 1150–1159.
[54] S. Glyn-Jones, A.J. Palmer, R. Agricola, A.J. Price, T.L. Vincent, H. Weinans, A.J. Carr, Osteoarthritis, Lancet 386 (2015) 376–387.
[55] A.R. Tellegen, I. Jansen, R. Thomas, H. de Visser, M. Kik, G. Grinwis, N. Woike, G. Mihov, P. Emans, B. Meij, L. Creemers, M. Tryfonidou, Controlled release of celecoxib inhibits inflammation, bone cysts and osteophyte formation in a pre-clinical model of osteoarthritis, Drug Deliv. 25 (2018) 1438–1447.